Calculation of glass forming ranges in Al–Ni–RE (Ce, La, Y) ternary alloys and their sub-binaries based on Miedema's model

S.P. Sun [a,b], D.Q. Yi [a,b,*], H.Q. Liu [a,b], B. Zang [a,b], Y. Jiang [a,b]

[a] School of Material Science and Engineering, Central South University, Changsha, 410083, China
[b] Key Laboratory of Non-ferrous Materials, Ministry of Education, Central South University, Changsha, 410083, China

ABSTRACT

A method based on the semi-empirical Miedema's and Toop's model for calculating the glass forming range of a ternary alloy system was systematically described. The method is superior to conventional models by considering the effect of the thermodynamic asymmetric component when dealing with a ternary alloy system. Using this method, the glass forming ranges of Al–Ni–RE (Ce, La, Y) systems and their sub-binaries were successfully predicted. The mixing enthalpy and mismatch entropy were calculated, and their effects on the glass forming abilities of Al–Ni–RE (Ce, La, Y) systems were also discussed. The glass forming abilities of Al–Ni–Ce, Al–Ni–La and Al–Ni–Y are found to be close. The calculated glass forming ranges agree with experiments well. Meanwhile, the enthalpy change from amorphous phase to solid solution in the glass forming ranges was calculated, and the results suggest that those alloys close to the Ni–RE sub-binary system have higher glass forming abilities.

© 2010 Elsevier B.V. All rights reserved.

1. Introduction

Al-based amorphous alloys have attracted considerable attention in recent years due to their outstanding mechanical and physical properties such as high mechanical strength, good corrosion resistance, and unique magnetic properties [1]. A great number of Al-based bulk metallic glass alloys have been developed using gas atomization, melt spinning, laser melting process and mechanical alloying [2]. However, the low thermal stability and poor ductility of these alloys seriously limit their potential in many structural applications. In the last few years, there have been a lot of research efforts in attempts to achieve better ductility and thermal stability, especially on Al–TM–RE systems [3–7]. A typical Al–TM–RE system includes Al–Ni–RE (Al–Ni–Ce, Al–Ni–Y and Al–Ni–La, etc.), in which, Ni, one of transition metals (TM), is able to improve the glass forming ability compared to the binary Al–RE alloys.

Glass forming ability is crucial for multi-component bulk metallic glasses alloys. Since the discovery of amorphous alloys, many efforts [7–14] have been focusing on understanding the mechanisms of amorphization and optimizing the glass forming composition for a better glass forming ability. The optimal glass forming composition was often determined by either topological approach [10] or a combination of topological and thermodynamics approach [11]. Meanwhile, many criteria for evaluating the glass forming ability of an amorphous alloy have been proposed, including the confusion rule and the eutectic point rule. And some empirical parameters have been developed accordingly, such as γ [12], γ^* [13] and δ [14]. Surprisingly, Al-based glasses, especially with rare earth elements, provide an important exception from this generality, i.e. they do not follow these general rules [2]. However, it is rarely found in the literature about the thermodynamic description for the Al-based glasses with rare earth additives. Many thermodynamic data are still not available up to now, possibly due to the technical difficulties, constituent complexity, experimental expenses and time consumption.

Theoretical approaches have been resorted to predict thermodynamic properties. Especially, Miedema's model [15] has been used to calculate the standard formation enthalpies of intermetallics [16,17] and liquid alloys [18], to predict phase-diagram thermodynamics [19,20], phase stability of mechanical alloying [21,22], glass forming abilities [23–26], and even interfacial behaviors [27]. In some earlier studies [24–26], glass forming ranges of ternary alloys have been calculated by comparing the formation enthalpies between amorphous and crystalline states using Miedema's model, and some interesting results have been obtained. However, there has been no mention on the effects of the asymmetric components when extrapolating from constitutive binary systems to ternary systems.

* Corresponding author at: School of Material Science and Engineering, Central South University, Changsha, 410083, China. Tel.: +86 731 88830263; fax: +86 731 88836320.
E-mail address: yioffice@mail.csu.edu.cn (D.Q. Yi).

Table 1
The values of parameters used in the calculations.

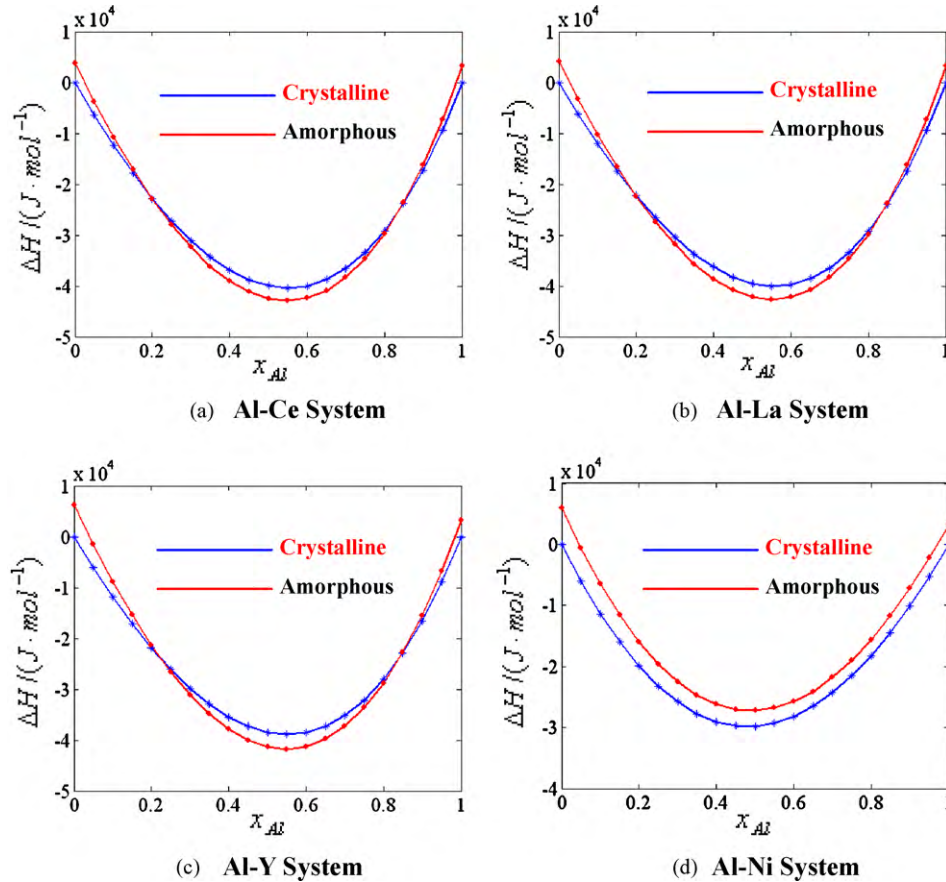| Element	T_i^m (K)	$V^{2/3}$ (cm^2)	$n_{ws}^{1/3}$ (d.u.)	ϕ/V	α/β	μ_i (GPa)	V_i (m^3)	K_i (GPa^{-1})
Al	933.25	4.64	1.39	4.20	1.9	26.2	10.0×10^{-6}	0.01385
Ni	1726	3.52	1.75	5.20	1.0	76.0	6.59×10^{-6}	0.00538
La	1193	7.98	1.18	3.17	0.7	14.9	20.73×10^{-6}	0.0412
Y	1799	7.34	1.21	3.20	0.7	25.5	19.8×10^{-6}	0.0273
Ce	1071	7.76	1.19	3.18	0.7	13.5	20.67×10^{-6}	0.0418

Fig. 1. Enthalpy–composition diagrams of binary (a) Al–Ce, (b) Al–La, (c) Al–Y and (d) Al–Ni systems.

In this paper, we propose to use Toop's model [28], an asymmetrical geometric model, to consider the asymmetric component effects and avoid the integration operation in the model of Chou [29], and calculate the glass forming ranges of Al–Ni–RE (La, Y, Ce) systems and its sub-binaries. The mixing enthalpy, the mismatch entropy, and the enthalpy change due to the amorphous-solid solution transition were also calculated, and compared with experiments.

2. Methodology

2.1. Miedema's semi-empirical model

Miedema et al. [15] proposed a so-called macroscopic atom picture to predict formation enthalpies of binary systems, which is a natural extension of Pauling's scheme of formation enthalpies of alloys and compounds. According to Miedema's approach, a binary alloy or intermetallics is assumed to be composed of Wigner–Seitz cells. When atoms A and B contact each other in the alloy, the alloying effect of the boundaries needs to be smoothed. The formation enthalpy in a binary alloy system consists of a negative contribution from the electronegativity difference between the two components, a positive contribution from difference in electron densities of the two components, and a correction of hybridization if one component is a transition element [30]. To be specific, the formation enthalpy ΔH_{AB} in a binary alloy system can be described as

$$\begin{cases} \Delta H_{AB} = f_{AB} \dfrac{x_A[1 + \mu_A x_B(\phi_A - \phi_B)] \times x_B[1 + \mu_B x_A(\phi_B - \phi_A)]}{x_A V_A^{2/3}[1 + \mu_A x_B(\phi_A - \phi_B)] + x_B V_B^{2/3}[1 + \mu_B x_A(\phi_B - \phi_A)]} & \text{(Disordered alloy)} \\[2mm] (\Delta H_{AB})_{order} = \Delta H_{AB} \times \left[1 + \gamma \times \left(\dfrac{V_A^{2/3} V_B^{2/3} \Delta H_{AB}}{f_{AB} \times \{x_A V_A^{2/3}[1 + \mu_A x_B(\phi_A - \phi_B)] + x_B V_B^{2/3}[1 + \mu_B x_A(\phi_B - \phi_A)]\}}\right)^2\right] & \text{(Ordered alloy)} \end{cases}$$

(1-a)

$$f_{AB} = 2pV_A^{2/3}V_B^{2/3} \times \frac{(q/p)(\Delta n_{ws}^{1/3})^2 - (\Delta \phi)^2 - a(r/p)}{(n_{ws}^{1/3})_A^{-1} + (n_{ws}^{1/3})_B^{-1}},$$

(1-b)

where $x_i, V_i, \phi_i, (n_{ws})_i (i = A, B)$ is mole fraction, mole volume, electronic density at the Wigner–Seitz cell boundary and electron chemical potential of each component, respectively. p, q, r, a, γ and μ_i are all empirical parameters, in which $q/p = 9.4, a = 0.73$ for a liquid alloy, 1 for a solid alloy if one component is a transition element, or 0 otherwise, and $\gamma = 5$ for a short-range ordered alloy or 8 for a long-range ordered
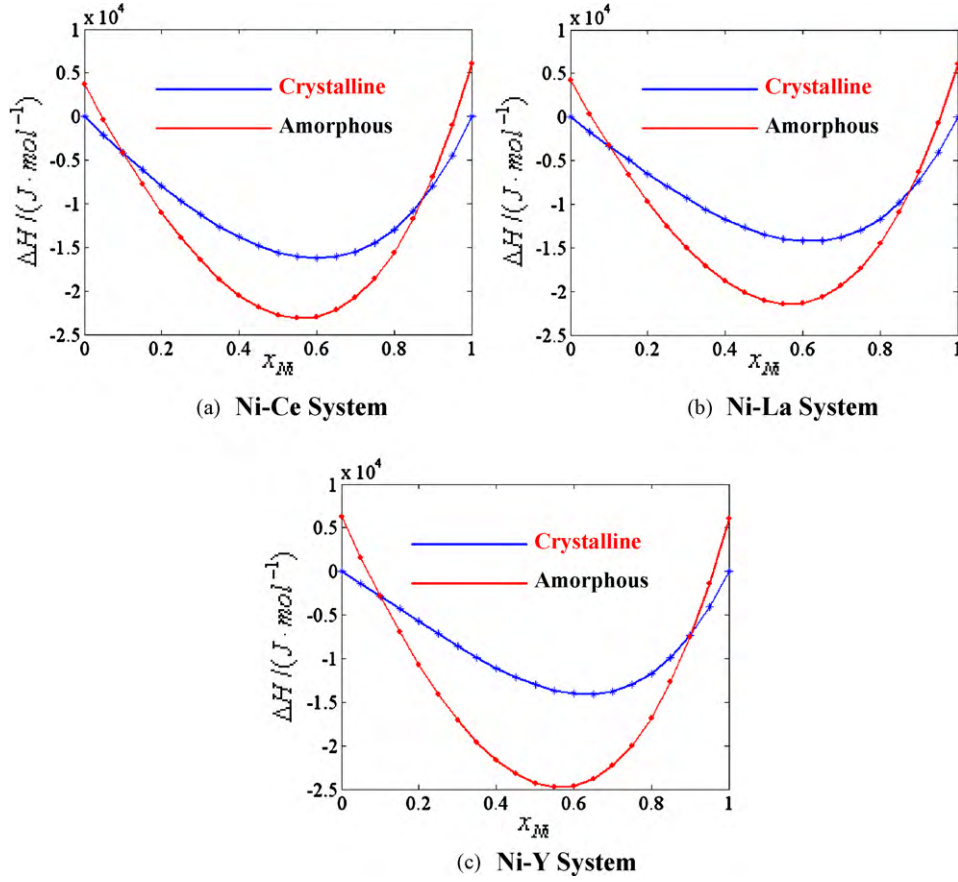
Fig. 2. Enthalpy–composition diagrams of ternary (a) Ni–Ce, (b) Ni–La and (c) Ni–Y systems.

alloy, respectively. The description of all above parameters can be referred to Refs. [15,30].

2.2. Glass forming ranges of binary alloys

An amorphous phase would be favored only if its free energy is lower than its solid solution counterpart. In this paper, we use Miedema's semi-empirical model to calculate the enthalpy–composition diagrams for both amorphous phases and their crystalline solid solution counterparts. The driving force for amorphization is dominated mainly by the enthalpy change, we hence ignore the entropy contribution to the free energy.

The formation enthalpy of a crystalline solid solution can be calculated as

$$\Delta H^{\text{cryst}} = \Delta H^{\text{chem}} + \Delta H^{\text{elast}} + \Delta H^{\text{struct}}, \tag{2}$$

where ΔH^{chem} is the chemical contribution due to the mixing of two components, ΔH^{elast} is the elastic contribution due to atom-size mismatch, and ΔH^{struct} is the structural contribution due to valence and crystal structure difference of two components, respectively.

ΔH^{chem} can be calculated by Eq. (1). The elastic mismatch energy, ΔH^{elast}, can be assessed by the following equations:

$$\Delta H^{\text{elast}} = x_A x_B (x_A \Delta H^{\text{elast}}_{\text{B in A}} + x_B \Delta H^{\text{elast}}_{\text{A in B}}), \tag{3}$$

where $\Delta H^{\text{elast}}_{\text{i in j}}$ (i, j = A, B) is the atom-size mismatch contribution to the solution enthalpy in a binary system, and can be written as [31]

$$\Delta H^{\text{elast}}_{\text{A in B}} = \frac{2\mu_B (V_A^* - V_B^*)^2}{3V_B^* + 4\mu_B K_A V_A^*}. \tag{4}$$

Here, μ_B is the shear modulus of the solvent, K_A is the compressibility of the solute, V_A^* and V_B^* are the molar volumes of the solute and the solvent, respectively, and can be evaluated as

$$(V_i^*)^{2/3} = V_i^{2/3}[1 + \mu_i(\phi_i - \phi_j)] \quad (i, j = A, B). \tag{5}$$

The contribution of formation enthalpy from structural difference has minimal effect, and thus can be neglected [26].

$$\Delta H^{\text{struct}} \approx 0 \tag{6}$$

For an amorphous alloy, the elastic contribution is absent but an additional topological term due to the amorphous nature has to be considered. The formation enthalpy of the amorphous phase can be expressed as

$$\Delta H^{\text{amorph}} = \Delta H^{\text{chem}} + \Delta H^{\text{topol}}, \tag{7}$$

where ΔH^{chem} and ΔH^{topol} are formation enthalpies of chemical and topological contributions, respectively. ΔH^{chem} can be calculated by Eq. (1), while ΔH^{topol} reflects the topological disorder in the amorphous state and can be estimated as

$$\Delta H^{\text{topol}} = 3.5 \times 10^{-3} \sum_i (x_i T_i^m) \tag{8}$$

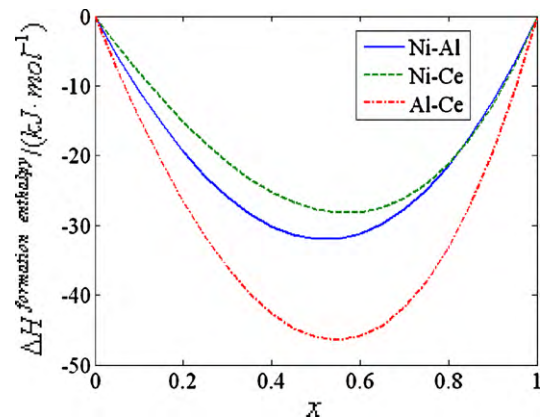where T_i^m is the melting temperature of component i.

Fig. 3. Variation of formation enthalpy of the Ni–Al, Ni–Ce and Al–Ce binary boundary alloys.
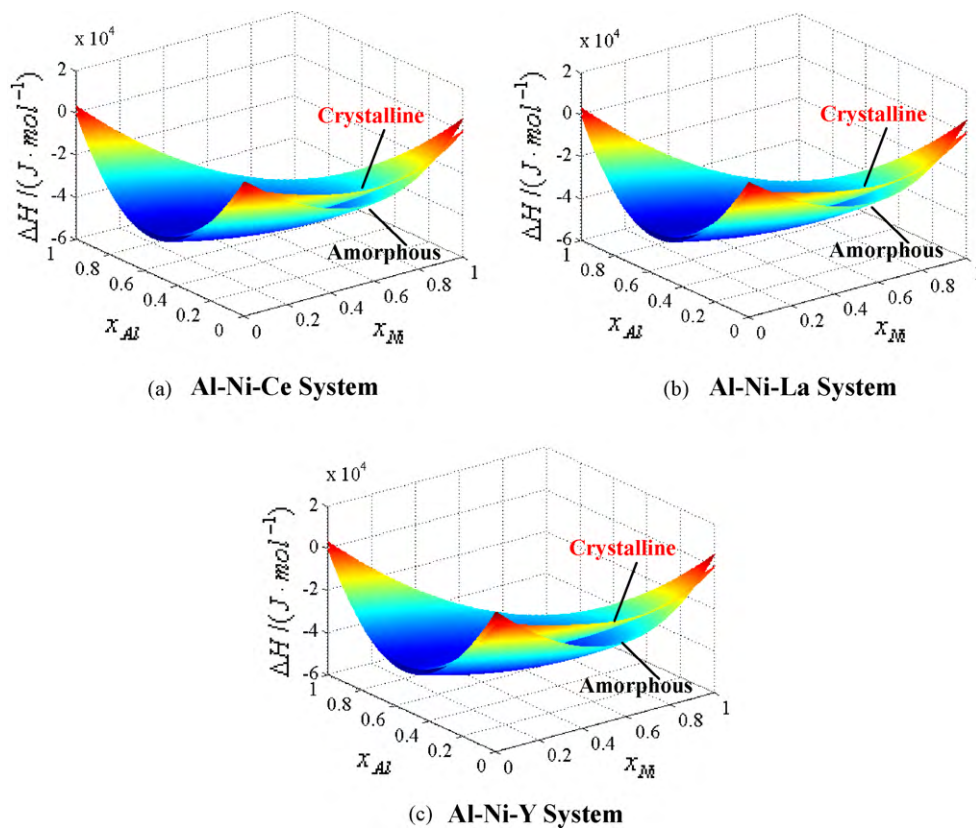
Fig. 4. Determination of glass forming abilities of ternary (a) Al–Ni–Ce, (b) Al–Ni–La, and (c) Al–Ni–Y systems based on the calculated enthalpy–composition relations.
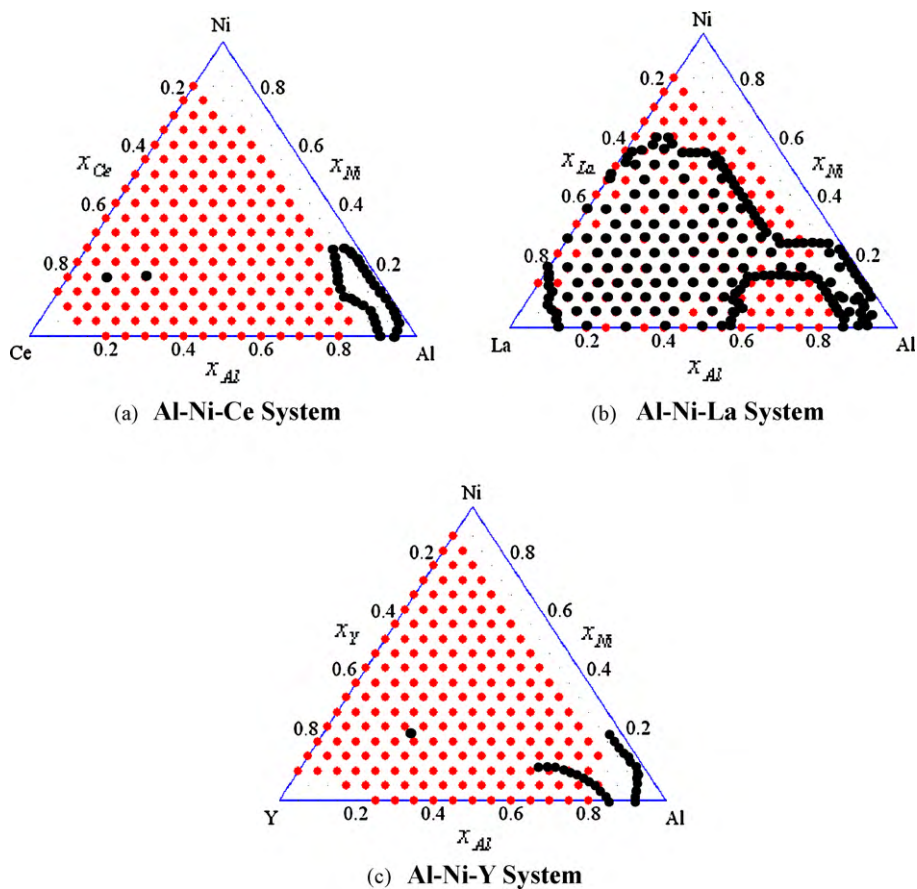

Fig. 5. Predicted and experimentally determined composition ranges for glass formation in (a) Al–Ni–Ce, (b) Al–Ni–La, and (c) Al–Ni–Y alloy systems.
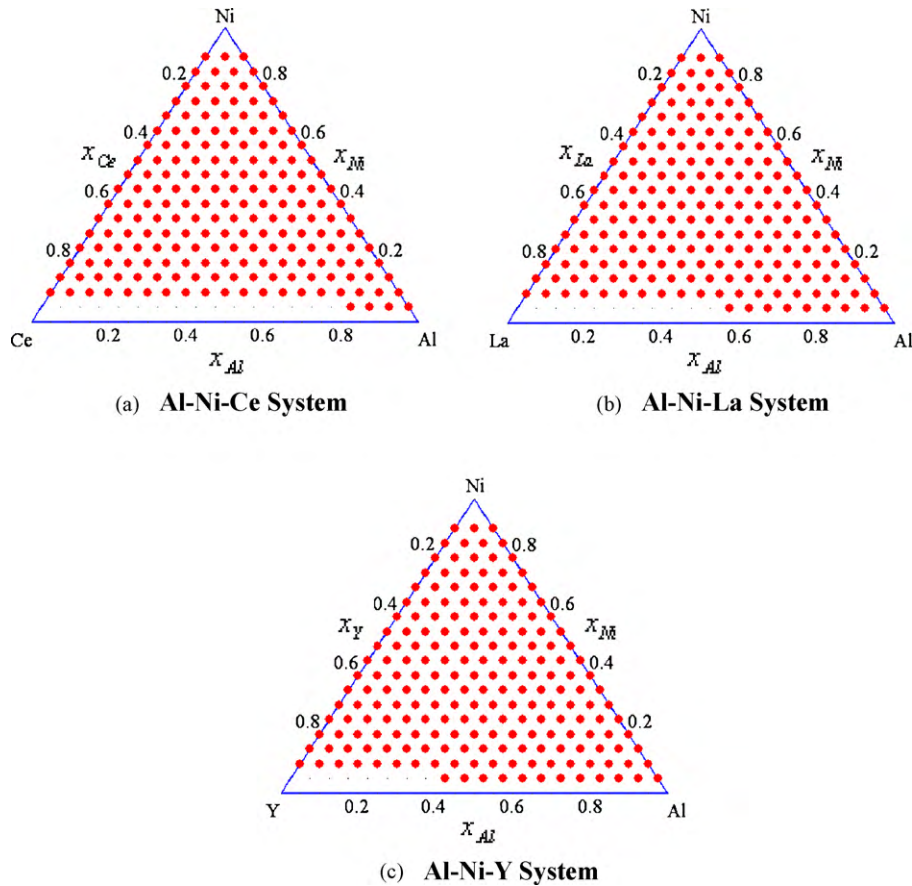
(a) **Al-Ni-Ce System**

(b) **Al-Ni-La System**

(c) **Al-Ni-Y System**

Fig. 6. Glass forming ranges of ternary (a) Al–Ni–Ce, (b) Al–Ni–La, and (c) Al–Ni–Y systems by a non-Toop's model in Ref. [26].

2.3. Glass forming ranges of ternary alloys

The calculation method of the glass forming range of a ternary alloy is similar to that of a binary alloy. However, thermodynamic properties of a ternary system must be obtained by extrapolating from the three sub-binary systems. There are two categories of traditional models for extrapolating, the symmetrical (Kohler, Muggianu models) and the asymmetrical (Toop, Hillert models) [32]. The effect of the third element on the binary system was not included in the traditional symmetrical models, which led to large deviation of calculated values from experiments, especially when the three constituents have distinct physical properties.

We use Toop's model in present paper, to consider the effect of the third element and avoid tedious integration operation in the model of Chou [29]. However, the choice of asymmetric constituent is not straightforward in Toop's model, and need to be adjusted by one's experience. Yan et al. [33] and Qiao et al. [34] have proposed a criterion of judging the asymmetric component in the ternary system, where the common component in two sub-binary systems with thermodynamic similarities should be chosen as the asymmetric component.

Toop's model [28] can be expressed as

$$\Delta H_{ijk}^{chem} = \frac{x_j}{x_j + x_k} \Delta H_{ij}^{chem}(x_i, 1 - x_i) + \frac{x_k}{x_j + x_k} \Delta H_{ik}^{chem}(x_i, 1 - x_i)$$
$$+ (x_j + x_k)^2 \Delta H_{jk}^{chem}\left(\frac{x_j}{x_j + x_k}, \frac{x_k}{x_j + x_k}\right), \tag{9}$$

where i, j and k are the three components in a ternary system, x_i, x_j or x_k is the mole fraction of each component, ΔH_{ij}^{chem}, ΔH_{ik}^{chem}, ΔH_{jk}^{chem} and ΔH_{ijk}^{chem} are the chemical contributions of the three sub-binary systems and the ternary system, respectively.

Similarly the elastic enthalpies ΔH^{elast} of ternary solid solution can be also extrapolated from those of constitutive binary systems according to Eq. (9). ΔH^{topol} can be also obtained by Eq. (8), but here the constituent number is three.

3. Calculation results

3.1. Calculation of glass forming ranges of binary alloys

Thermodynamic parameters used in Miedema's model [30] for calculating formation enthalpies from electron structures are listed

in Table 1. The data of melting point, rigidity modulus, molar volume, and compressibility [35] for predicting elastic enthalpies are also given in Table 1.

The calculated enthalpy–composition diagrams of binary Al–Ce, Al–La, Al–Y and Al–Ni systems are given in Fig. 1. It can be seen that the forming ranges of amorphous phase in Al–Ce, Al–La and Al–Y systems are almost identical, and can be determined as 20–80 at.% Ce, 20–80 at.% La and 20–79 at.% Y, respectively. In Al–Ni binary system, the formation enthalpy of amorphous state is always higher than that of crystalline solid solution (Fig. 1d), suggesting no glass forming ability. The Al–Ce and Al–Y systems have not been experimentally studied in the entire composition range; while for the Al–La system the experimental glass forming range is rather wide, from 7 up to about 86 at.% La [36]. This is consistent well with our prediction (Fig. 1b). Ce and Y are believed to play similar roles as La, due to their very similar chemical properties and thermodynamics parameters.

The metallic glasses are configurationally frozen (supercooled) liquids and more prone to form at near deep-eutectic composition. Nevertheless, the amorphous phases of Al–Ce, Al–La and Al–Y alloys in Al-rich regions form in the composition ranges of 7–11 at.% Ce, 7–11 at.% La or 9–13 at.% Y respectively, a composition range between the eutectic point and $Al_{11}R_3$ (R = La, Ce) or Al_3R (R = Y) compounds [2]. These hypereutectic alloys tend to exhibit better glass formation abilities than the eutectic alloys. In fact, according to Al–RE binary phase diagrams, the glass forming ranges lie asymmetrically in the region of the phase diagram where the liquidus temperature rises steeply.

As mentioned above, Al–Ni binary alloys have no glass forming range. However, there was an experimental report of a partial-amorphous composition of Al–7 at.% Ni [2], where the alloy is a mixing of amorphous and crystalline microstructures. In fact, the

formation of glassy alloy by rapid solidification or mechanically alloying is affected by both thermodynamic and kinetic factors. The glass formation may sensitively depend on many kinetic factors, such as cooling rate, nucleation and growth. Even for an amorphous-impossible alloy from thermodynamics, sometimes one can still manage to obtain partial-amorphous structures by applying appropriate kinetic conditions. As it is well known, the glass state is just metastable.

The enthalpy–composition diagrams of Ni–Ce, Ni–La and Ni–Y systems are given in Fig. 2. It can also be seen that glass forming ranges of Ni–Ce, Ni–La and Ni–Y systems are very similar with the composition of 11–87, 11–87 or 10–90 at. % Ni, respectively. Only a few experimental data could be found in the literatures for Ni–RE based amorphous alloys. The amorphous phases of Ni–Ce and Ni–La binary alloys form only at the compositions of 50 at.% Ce [37], and 22, 33, 40 or 50 at.% La [38]. The amorphous compositional range of Ni–Y binary alloy is much wider: 8–32.5 at.% Y [39], which is almost fully located in our predicted range.

From Fig. 2, the enthalpy differences of Al–Ce, Al–La and Al–Y binary alloys are smaller than those of Ni–Ce, Ni–La and Ni–Y alloy systems. The enthalpy difference between the crystalline solid solution and the supercooled liquid states represents the driving force for crystallization; hence the glass formation abilities of Ni–Ce, Ni–La and Ni–Y systems are better than those of Al–Ce, Al–La and Al–Y alloys. This implies that Ni can improve the glass forming abilities of the binary Al–RE alloys.

3.2. Calculation of glass forming ranges of ternary alloys

As shown in Fig. 3, the formation enthalpy curves of Ni–Al and Ni–Ce sub-binaries are similar, but different to that of the Al–Ce sub-binary. According to our approach mentioned above, the Al–Ni–Ce ternary system is asymmetric, and Ni should be chosen as the asymmetric component in this asymmetric system. This is because that Ni not only has smaller molar volume and higher electronic density, but also has significantly different modulus parameters, compared to the other two components. Similarly, in Al–Ni–La and Al–Ni–Y systems, Ni should be selected as the asymmetric component too.

The glass forming ranges of Al–Ni–Ce, Al–Ni–La, and Al–Ni–Y ternary alloys can be determined by calculating and comparing the formation enthalpies between amorphous and crystalline alloys using Miedema's model. Fig. 4 shows the calculated formation enthalpies of the amorphous and the crystalline alloys in three-dimension. The axes for Ni and Al concentrations are given explicitly; an axis for Ce, La or Y is not necessary because its concentrations can be determined by the sum rule of $x_{Al} + x_{Ni} + x_{RE} = 1$. Only the regions where the amorphous enthalpy surface is located below than its crystalline counterpart shall be predicted as the glass forming range.

In Fig. 5, we further project the predicted glass forming range onto the Gibbs triangle which reflects thermodynamic characteristic of the ternary system. Each red dot represents a composition with a thermodynamically possible glass forming ability. The series of experimental results are also given as black dots in Fig. 5 for comparison. A number of experimental data are available for Al–Ni–La [40] but not for Al–Ni–Ce and Al–Ni–Y, expect their Al-rich corners [7,41,42].

The glass forming ranges of these sub-binaries in Al–Ni–RE systems (Fig. 5) match with the composition ranges calculated in Fig. 1 and Fig. 2. In Al–Ni–Ce system, the glass forms in the composition range of 0–80 at.% Al and 10–85 at.% Ce. In the composition range of 20–80 at.% Ce, the glass forming composition range extends from the Ni–Ce rich corner to the Al–Ce rich corner, suggesting that glass may form at any combination of Al and Ni. It is also noted that the glass forming ranges of Al–Ni–La and Al–Ni–Y systems are

very similar to that of Al–Ni–Ce system. Their large glass forming ranges can be related to their good glass forming abilities and high thermal stabilities of the supercooled liquids. As seen from Fig. 5, the glass composition range in Al–Ni–La system predicted on the basis of the Miedema's model agrees well with the experimental results, except at Al-rich corner. The large derivation at Al-rich corner can be also seen in the Al–Ni–Ce and Al–Ni–Y system, the reason for which is still not clear. Others' calculations using similar methods on Al–Ni–La and Al–Ni–Y can be found in Refs. [40] and [7]. Their results agree well with ours. One possible cause for the large deviation at Al-rich corner we can propose is: the predicted forming ranges of Al–RE binary systems were a little far away from the Al-rich region compared to experimental results, which might lead to the large deviation of calculated glass forming range of Al–Ni–RE ternary systems from experimental one at the Al-rich region when thermodynamic properties were extrapolated from constitutive binary systems according to Toop's model. It was found to be the case in Al–Ni–Zr alloys [43]. Nevertheless, more experimental data from the outside of Al-rich region is demanded, in order to verify our proposed cause, especially for the Al–Ni–Ce and Al–Ni–Y system.

It should be noted that our calculations cannot predict the coexistence of the amorphous and crystalline phases. In fact, these two-phase co-existing regions have been previously reported in experiments, for example Al–Ni system [2].

In present paper, Toop's model was used in extrapolating thermodynamic properties of ternary systems from three sub-binary systems. If neglecting the ternary interaction parameter, the glass forming ranges of ternary alloys cannot be appropriately predicted. As a comparison, the glass forming ranges of Al–Ni–RE (Ce, La, Y) ternary systems calculated by a non-Toop's model in Ref. [26] are given in Fig. 6.

Evidently, our calculated ranges are in better agreement with experiments than the results obtained by the non-Toop's approach in Ref. [26], for the latter totally ignored the effect of asymmetric constituent.

4. Further discussions

4.1. Mixing enthalpy of Al–Ni–RE (Ce, La, Y) ternary alloys

Table 2 lists the calculated mixing enthalpies of liquid phase with some specific Al–Ni–Ce amorphous compositions based on the present model and the available calculated values [41] by CALPHAD method for a comparison.

For both the CALPHAD and the present results, mixing enthalpies are sensitively dependent on compositions. The agreement between the two sets of calculated results is generally acceptable: the deviation is normally less than 20%, except only a few compositions. The same comparison has been also made for those typical intermetallic compounds in Al–Ni–Ce [41] in Table 3, and the similar agreement is observed. Table 4 compares the present results of Al–Ni–Y systems with experiments [44–47], showing an overall agreement. We can conclude that our approach from the combination of Miedema's and Toop's model is effective for predicting formation enthalpies and thermodynamic behaviors of Al–Ni–RE (Ce, La, Y) systems.

As we know, a high negative mixing enthalpy can help on macrostructural homogeneity without forming phase separation in an undercooled melt, and improve its thermodynamical stability [48]. This is a favorable condition for forming bulk metallic glass. We plot the mixing enthalpy contours of Al–Ni–RE (Ce, La, Y) ternary systems in Fig. 7, and note that the mixing enthalpies of Al–Ni–RE (Ce, La, Y) ternary systems range mainly from −5 to −45 kJ/mol. Recall that Takeuchi and Inoue [49] have calculated

Table 2
The mixing enthalpies for the liquid phases with specified Al–Ni–Ce compositions calculated by CALPHAD method and by present model.

No.	Composition (%)			$\Delta H_{CALPHAD}$ (kJ/mol-atom)	ΔH_{calc} (kJ/mol-atom)	$\left\| \Delta H_{calc} - \Delta H_{CALPHAD} \right\| / \Delta H_{CALPHAD}$ (%)
	Al	Ce	Ni			
1	94.7	2.6	2.6	−8.303	−8.684	4.583
2	96.3	1.6	2.1	−5.901	−5.876	0.420
3	65	15	20	−43.481	−38.940	10.443
4	70	15	15	−38.356	−36.700	4.317
5	60	10	30	−49.221	−37.962	22.874
6	61	10	29	−48.484	−37.652	22.341
7	70	10	20	−40.103	−33.880	15.518
8	75	10	15	−34.359	−31.039	9.663
9	80	10	10	−28.106	−27.683	1.505
10	85	10	5	−21.553	−23.825	10.541
11	89	10	1	−16.217	−20.386	25.705
12	89	8.6	2.4	−16.382	−19.351	18.124
13	82	8	10	−25.951	−24.781	4.508
14	85	7	8	−22.076	−21.609	2.116
15	80	6	14	−29.002	−24.768	14.600
16	84	6	10	−23.601	−21.644	8.292
17	85	6	9	−22.221	−20.812	6.340
18	86	6	8	−20.832	−19.960	4.186
19	87	6	7	−19.435	−19.088	1.786
20	88	6	6	−18.033	−18.196	0.903
21	65	5	30	−46.060	−32.705	28.995
22	75	5	25	−41.253	−22.962	44.338
23	80	5	15	−29.181	−23.963	17.882
24	85	5	10	−22.350	−19.985	10.583
25	87	5	8	−19.537	−18.250	6.585
26	90	5	5	−15.269	−15.498	1.501
27	80	4.4	15.6	−29.278	−23.465	19.856
28	85	4	11	−22.463	−19.126	14.856
29	86	4	10	−21.048	−18.264	13.227
30	78	3.5	18.5	−32.039	−24.152	24.618
31	88	2	10	−18.286	−14.633	19.978
32	72	10	18	−37.880	−32.806	13.395
33	75	15	10	−32.671	−33.953	3.925
34	64	6	30	−46.786	−33.872	27.602

Table 3
The formation enthalpies for some intermetallic compounds in Al–Ni–Ce system calculated by CALPHAD method and by present model.

No.	Ternary phase	$\Delta H_{CALPHAD}$ (kJ/mol-atom)	ΔH_{calc} (kJ/mol-atom)	$\left\| \Delta H_{calc} - \Delta H_{CALPHAD} \right\| / \Delta H_{CALPHAD}$ (%)
1	Al_4CeNi	−47.08	−44.60	5.26
2	Al_5CeNi_2	−51.29	−45.51	11.28
3	$Al_{23}Ce_4Ni_6$	−46.14	−39.46	14.49

Table 4
Calculated and experimentally measured enthalpies of formation for some intermetallic compounds in the Al–Ni–Y system.

No.	Intermetallic	ΔH_{exp} (kJ/mol-atom)	ΔH_{calc} (kJ/mol-atom)	$\left\| \Delta H_{calc} - \Delta H_{exp} \right\| / \Delta H_{exp}$ (%)
1	$Al_{19}Ni_5Y_3$	−50.1	−38.19	23.78
2	$Al_{23}Ni_6Y_4$	−50.6	−39.38	22.18
3	Al_4NiY	−54.0	−44.60	17.40
4	Al_3NiY	−59.8	−51.15	14.46
5	Al_2NiY	−62.8	−58.65	6.61
6	Al_3Ni_2Y	−62.8	−56.46	10.10
7	$AlNiY$	−59.0	−62.12	5.28
8	$AlNi_2Y_2$	−54.1	−56.59	4.60
9	$Al_2Ni_6Y_3$	−48.5	−58.55	20.73
10	$AlNi_8Y_3$	−37.9	−47.84	26.23
11	Al_3Y	−46.4	−45.17	2.64
12	Al_2Y	−53.5	−54.88	2.57
13	Al_2Y_3	−46.9	−54.25	15.67
14	$AlNi_3$	−37.6	−33.47	10.99
15	$AlNi$	−58.0	−47.51	18.08
16	Al_3Ni_2	−57.6	−42.55	26.13
17	Al_3Ni	−37.7	−28.00	25.72
18	Y_2Ni_{17}	−13.11	−16.64	26.93
19	YNi_5	−21.28	−26.47	24.39
20	YNi_4	−25.19	−31.38	24.57
21	Y_2Ni_7	−27.83	−34.35	23.44
22	YNi_3	−29.06	−37.65	29.57
23	YNi_2	−31.30	−44.26	41.41
24	YNi	−35.38	−43.06	21.71
25	Y_3Ni_2	−35.26	−36.18	2.62
26	Y_3Ni	−33.31	−22.92	31.20

(a) **Al-Ni-Ce System**

(b) **Al-Ni-La System**
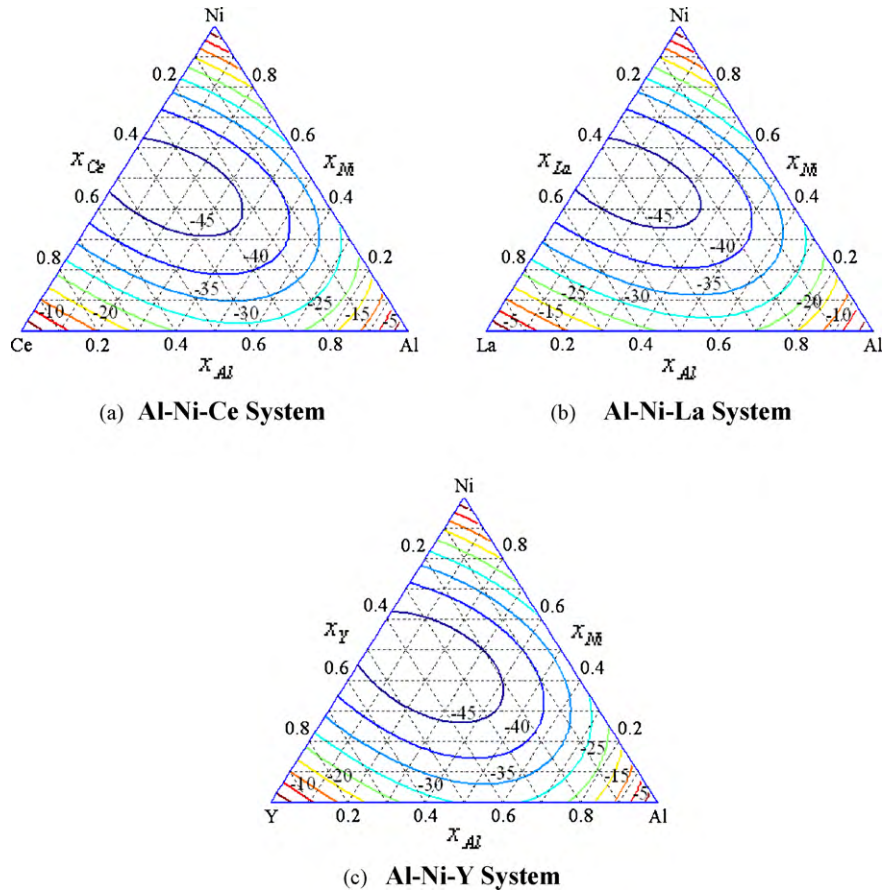

(c) **Al-Ni-Y System**

Fig. 7. The mixing enthalpy contours for the (a) Al–Ni–Ce, (b) Al–Ni–La, and (c) Al–Ni–Y alloy systems. The figures on the contour are in kJ/mol.

the mixing enthalpies of 6450 alloys in 351 ternary amorphous systems to be ranging from 0 and −55 kJ/mol, with an average value of −33 kJ/mol. This suggests that the Al–Ni–RE (Ce, La, Y) ternaries might have potentially high glass forming ability. Tang et al. [41] also proposed that a high negative mixing enthalpy might enhance the tendency to form chemically short-range ordering and hence improve the glass forming abilities of Al–Ni–Ce alloys.

4.2. Effect of mismatch entropy in Al–Ni–RE (Ce, La, Y) ternary alloys

Most of bulk amorphous alloys commonly have multi-components with significantly different atomic sizes. In fact, atomic size difference is a very important factor for predicting the formation of amorphous. The atomic size mismatch has been considered in calculating the elastic mismatch enthalpy, but its effect on the mismatch entropy has been totally neglected. According to an empirical derivation [50], the mismatch entropy normalized by Boltzmann's constant can be calculated by the following equation:

$$\frac{S_\sigma}{k_B} = \frac{3}{2}(\zeta^2 - 1)y_1 + \frac{3}{2}(\zeta^2 - 1)y_2$$
$$- \left\{ \frac{1}{2}(\zeta - 1)(\zeta - 3) + \ln\zeta \right\}(1 - y_3), \tag{10}$$

where k_B is Boltzmann's constant and $\zeta = 1/(1 - \xi)$. $\xi = 0.64$ for a dense random packing. The dimensionless parameters y_1, y_2 and y_3 are defined according to following equations:

$$y_1 = \frac{1}{\sigma^3}\sum(d_i + d_j)(d_i - d_j)^2 x_i x_j \tag{11}$$

$$y_2 = \frac{\sigma^2}{(\sigma^3)^2}\sum(d_i d_j)(d_i - d_j)^2 x_i x_j \tag{12}$$

$$y_3 = \frac{(\sigma^2)^3}{(\sigma^3)^2} \tag{13}$$

$$\sigma^k = \sum x_i d_i^k \quad (k = 2, 3). \tag{14}$$

Here d_i and d_j are the atomic diameters of i and j elements.

The contours of the normalized mismatch entropies of Al–Ni–RE (Ce, La, Y) ternary systems have been obtained and shown in Fig. 8.

From Fig. 8, the normalized mismatch entropies of Al–Ni–RE (Ce, La, Y) ternary systems range from 0.1 to 0.9, especially 0.1 to 0.3 near the Al-rich corner. According to Bhatt et al. [11] and Basu et al. [26], the calculated normalized mismatch entropies of amorphous Al–Cu–Zr and Al–Ni–Zr ternaries range from 0.1 and 0.3. Takeuchi and Inoue [49] also proposed that the average normalized mismatch entropy value of ternary amorphous systems was ∼0.33 based on their calculations on 6450 amorphous alloys in 351 ternary systems. Combining with our earlier analyses on mixing enthalpies, one can naturally deduce that the Al-rich Al–Ni–RE (Ce, La, Y) ternaries has strong intention to form amorphous phases. This may help explain the earlier controversy as shown in Fig. 5 that the experimentally observed Al–Ni–RE amorphous alloys were mainly located in the Al-rich region, especially for the Al–Ni–Ce and Al–Ni–Y systems, while the mixing enthalpy-only calculations failed to predict. We hence believe that the deviation of our theoretical predictions in Fig. 5 from experiments is largely due to the neglect of mismatch entropies, besides the possible cause mentioned in Section 3.2.
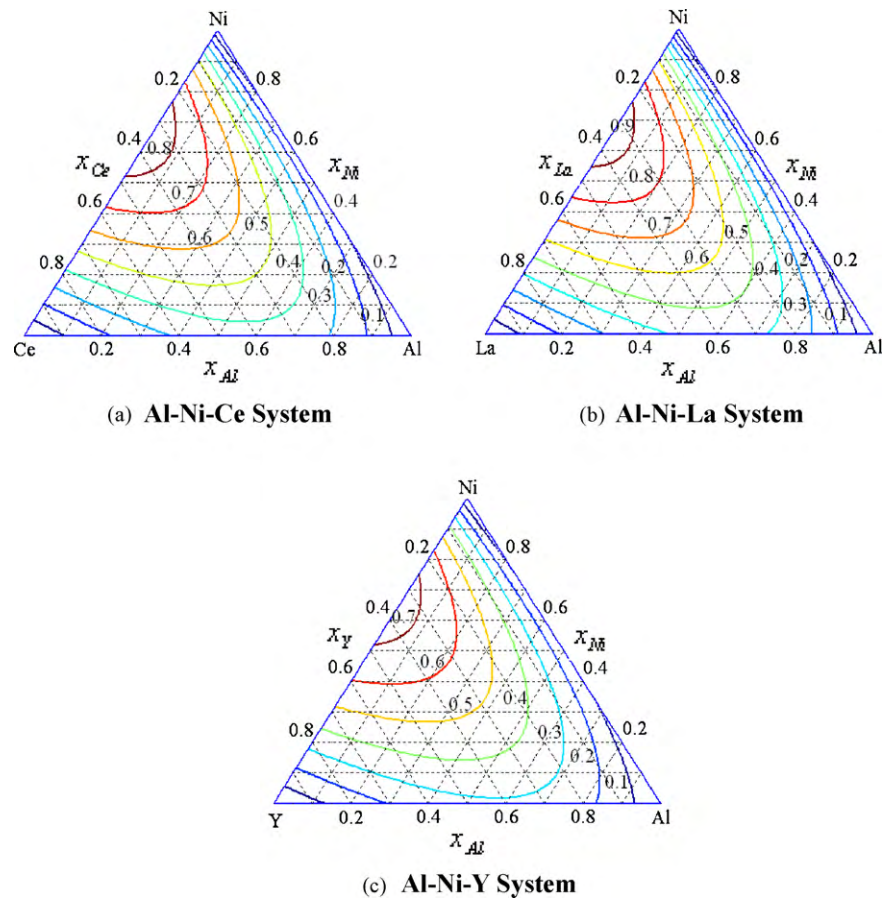
(a) **Al-Ni-Ce System**

(b) **Al-Ni-La System**

(c) **Al-Ni-Y System**

Fig. 8. The normalized mismatch entropy contours (S_σ/k_B) for the (a) Al–Ni–Ce, (b) Al–Ni–La, and (c) Al–Ni–Y alloy systems.

Table 5 shows the atomic radius, electronic structure, crystal structure and atomic size difference of these elements. Based on a large number of experiments and calculations, Inoue [1] concluded that a multi-component alloy with three or more elements need an at least 12% atomic radius difference and a negative value of mixing heat, in order to form its amorphous phase. From Table 5, and Fig. 7, it is evident that the Al–Ni–RE ternary systems have large atomic size difference and negative mixing enthalpy, and its high glass forming ability is hence expectable. The atomic size difference between Al and Ni is only 11%, and accordingly an Al–Ni binary alloy shall hardly form its amorphous phase. This seems to be consistent well with experimental observations.

4.3. Glass forming ability and enthalpy change of Al–Ni–RE (Ce, La, Y) ternary alloys

The enthalpy difference between crystalline solid solution and supercooled liquid, providing the driving force for amorphization, could be calculated as

$$\Delta H^{\text{enthalpy change}} = \Delta H^{\text{cryst}} - \Delta H^{\text{amorph}} \qquad (15)$$

Fig. 9 plots the enthalpy changes due to glass formation for the three Al–Ni–RE systems. It reveals that the amorphization ability is strongly dependent on its composition. In Fig. 9, the highest enthalpy change appears close to the Ni–RE boundary rather than near the Al-rich corner. This indicates that these alloys close to the Ni–RE sub-binary system have higher thermal stabilities. The values of enthalpy change reduce with the increasing Al content, resulting in the decrease of driving force for amorphization. Nevertheless, the Al-rich alloys often have excellent ductility, and thus have been also a focus of many studies [51–54].

As mentioned above, a higher enthalpy change implies a higher driving force for amorphrization and hence a higher glass forming ability. From Fig. 9, the sequence of enthalpy change can be determined as

$$\Delta H^{\text{enthalpy change}}_{\text{Al−Ni−Y}} > \Delta H^{\text{enthalpy change}}_{\text{Al−Ni−La}} > \Delta H^{\text{enthalpy change}}_{\text{Al−Ni−Ce}} \qquad (16)$$

The glass forming abilities of these systems would follow the same sequence, which is in accordance with the experimental results [2].
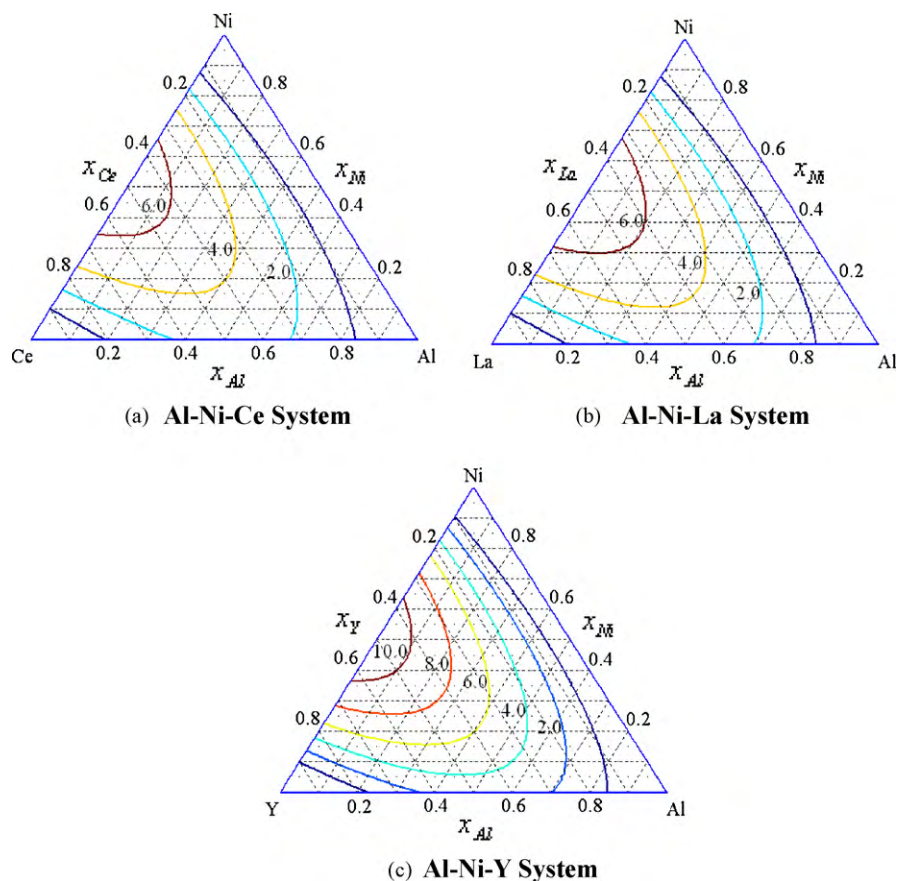
Table 5
Atomic radius, atomic size difference, electronic structure and crystal structure of the elements.

Elements	Atomic radius	Electronic structure	Crystal structure	$|r_i - r_{Al}|/r_{Al}$	$|r_i - r_{Ni}|/r_{Ni}$
Al	1.82	$3s^2 3p^1$	fcc	0	11.0%
Ni	1.62	$3d^8 4s^2$	fcc	11.0%	0
La	2.74	$5d^1 6s^2$	hcp	50.5%	69.1%
Y	2.27	$4d^1 5s^2$	hcp	24.7%	40.1%
Ce	2.70	$4f^1 5d^1 6s^2$	fcc	48.4%	66.7%

Fig. 9. The enthalpy change contours for the (a) Al–Ni–Ce, (b) Al–Ni–La, and (c) Al–Ni–Y alloy systems. The figures on the contour are in kJ/mol.

5. Conclusions

A method based on semi-empirical Miedema's and Toop's model to predict the glass forming range of a ternary alloy system has been systematically described, and applied to Al–Ni–RE (Ce, La, Y) systems. The method is superior to conventional models by considering the effect of the thermodynamic asymmetric component. The glass forming ranges of Al–Ni–RE (Ce, La, Y) systems and its sub-binaries have been calculated using this method with including mixing enthalpies and mismatch entropies. Our calculations are in well agreement with experiments. The calculated enthalpy changes suggest that those alloys close to the Ni–RE sub-binary system should have a higher glass forming abilities. Conceptually, this method can be used to predict the glass forming range and glass forming abilities of any binary, ternary and even multi-component system. Nevertheless, our model cannot predict the co-existing region of amorphous and crystalline phases, as already observed in some experiments. A set of empirical parameters is required in the method, and the calculation precision is hence limited. A more accurate model is desired to be developed in our future work.

Acknowledgement

References

[1] A. Inoue, Acta Mater. 48 (2000) 279–306.
[2] A. Inoue, Prog. Mater. Sci. 43 (1998) 365–520.
[3] G.H. Li, W.M. Wang, X.F. Bian, J.T. Zhang, R. Li, L. Wang, J. Alloys Compd. 478 (2009) 745–749.
[4] F. Sun, T. Gloriant, J. Alloys Compd. 477 (2009) 133–138.
[5] J.G. Lin, W.W. Wang, X.Q. Wu, J.H. Lei, S. Yin, J. Alloys Compd. 478 (2009) 763–766.
[6] Z. Huang, J. Li, Q. Rao, Y. Zhou, J. Non-Cryst. Solids 355 (2009) 154–158.
[7] Y.K. Kim, J.R. Soh, D.K. Kim, H.M. Lee, J. Non-Cryst. Solids 242 (1998) 122–130.
[8] J. Guo, X. Bian, X. Li, C. Zhang, Intermetallics 18 (2010) 933–937.
[9] P.K. Ray, M. Akinc, M.J. Kramer, J. Alloys Compd. 489 (2010) 357–361.
[10] D.B. Miracle, O.N. Senkov, Mater. Sci. Eng. A 347 (2003) 50–58.
[11] J. Bhatt, W. Jiang, X. Junhai, W. Qing, C. Dong, B.S. Murty, Intermetallics 15 (2007) 716–721.
[12] Z.P. Lu, C.T. Liu, Acta Mater. 50 (2002) 3501–3512.
[13] L. Xia, S.S. Fang, Q. Wang, Y.D. Dong, C.T. Liu, Appl. Phys. Lett. 88 (2006) 171905.
[14] Q. Chen, J. Shen, D. Zhang, H. Fan, J. Sun, D.G. McCartney, Mater. Sci. Eng. A 433 (2006) 155–160.
[15] A.R. Miedema, P.F. de Châtel, F.R. de Boer, Physica B+C 100 (1980) 1–28, doi:10.1016/0378-4363(80)90054-6.
[16] S.V. Meschel, P. Nash, Xing-Qiu Chen, J. Alloys Compd. 492 (2010) 105–115.
[17] J.F. Fernandez, J.R. Ares, F. Cuevas, J. Bodega, F. Leardini, C. Sánchez, Intermetallics 18 (2010) 233–241.
[18] H.W. Yang, D.P. Tao, X.M. Yang, Q.M. Yuan, J. Alloys Compd. 480 (2009) 625–628.
[19] Z.H. Long, H.S. Liu, Z.P. Jin, J. Alloys Compd. 479 (2009) 262–267.
[20] Y. Djaballah, A. Pasturel, A. Belgacem-Bouzida, J. Alloys Compd. 497 (2010) 74–79.
[21] G. Gonzalez, A. Sagarzazu, D. Bonyuet, L. D'Angelo, R. Villalba, J. Alloys Compd. 483 (2009) 289–297.
[22] S. Sheibani, S. Heshmati-Manesh, A. Ataie, J. Alloys Compd. 495 (2010) 59–62.
[23] G.W. Qin, B. Yang, N. Xiao, Y.P. Ren, M. Jiang, X. Zhao, K. Oikawa, Thin Solid Films 517 (2009) 2984–2987.
[24] T.L. Wang, W.C. Wang, J.H. Li, B.X. Liu, J. Alloys Compd. 493 (2010) 154–157.
[25] R. Hojvat de Tendler, M.R. Soriano, M.E. Pepe, J.A. Kovacs, E.E. Vicente, J.A. Alonso, Intermetallics 14 (2006) 297–307.
[26] J. Basu, B.S. Murty, S. Ranganathan, J. Alloys Compd. 465 (2008) 163–172.
[27] F. Sommer, R.N. Singh, E.J. Mittemeijer, J. Alloys Compd. 467 (2009) 142–153.
[28] G.W. Toop, Trans. Metall. Soc. AIME 233 (1965) 850–855.
[29] K.C. Chou, CALPHAD 19 (1995) 315–325.
[30] F.R. de Boer, R. Boom, W.C.M. Mattens, A.R. Miedema, A.K. Niessen, Cohesion in Metals, North-Holland, Amsterdam, 1988.
[31] A.K. Niessen, A.R. Miedema, Ber. Bunsenges, Phys. Chem. 87 (1983) 717–725.
[32] D. Manasijević, D. Živković, Ž. Živković, CALPHAD 27 (2003) 361–366.
[33] L. Yan, S. Zheng, G. Ding, G. Xu, Z. Qiao, CALPHAD 31 (2007) 112–119.
[34] Z.Y. Qiao, X. Xing, M. Peng, A. Mikula, J. Phase Equilib. 17 (1996) 502–507.

[35] E.A. Brandes, G.B. Brook, Smithells metals reference book, 7th ed., Butterworth-Heinemann, Oxford, United Kingdom, 1992.

[36] A. Inoue, T. Zhang, T. Masumoto, J. Non-Cryst. Solids 156–158 (1993) 473–480.

[37] F. Wastin, K. Sumiyama, T. Hihara, H. Yamauchi, Y. Homma, M. Sakurai, K. Suzuki, Physica B 186–188 (1993) 563–565.

[38] U.I. Chung, J.Y. Lee, J. Non-Cryst. Solids 110 (1989) 203–210.

[39] A. Fujita, T.H. Chiang, N. Kataoka, K. Fukamichi, J. Phys. Soc. Japan 62 (1993) 2579–2582.

[40] A. Inoue, A. Takeuchi, Mater. Sci. Eng. A 375–377 (2004) 16–30.

[41] C. Tang, Y. Du, J. Wang, H. Zhou, L. Zhang, F. Zheng, J. Lee, Q. Yao, Intermetallics 18 (2010) 900–906.

[42] Y. Wang, C.H. Shek, J. Qiang, C. Dong, S. Pang, T. Zhang, J. Alloys Compd. 434–435 (2007) 167–170.

[43] T. Shindo, Y. Waseda, A. Inoue, Mater. Trans. JIM 43 (2002) 2502–2508.

[44] W.J. Golumbfskie, R. Arroyave, D. Shin, Z.-K. Liu, Acta Mater. 54 (2006) 2291–2304.

[45] V.S. Timofeev, A.A. Turchanin, A.A. Zubkov, I.A. Tomilin, Thermochim. Acta 299 (1997) 37–41.

[46] F.Z. Chrifi-Alaoui, M. Nassik, K. Mahdouk, J.C. Gachon, J. Alloys Compd. 364 (2004) 121–126.

[47] P.R. Subramanian, J.F. Smith, Metall. Mater. Trans. B 16 (1985) 577–584.

[48] A. Zhu, G.J. Shiflet, D.B. Miracle, Scripta Mater. 50 (2004) 987–991.

[49] A. Takeuchi, A. Inoue, Mater. Trans. JIM 41 (2000) 1372–1378.

[50] G.A. Mansoori, N.F. Carnahan, K.E. Starling, T.W. Leland, J. Chem. Phys. 54 (1971) 1523–1525.

[51] C.T. Rios, S. Suriñach, M.D. Baró, C. Bolfarini, W.J. Botta, C.S. Kiminami, J. Non-Cryst. Solids 354 (2008) 4874–4877.

[52] Z. Huang, J. Li, Q. Rao, Y. Zhou, J. Non-Cryst. Solids 354 (2008) 1671–1677.

[53] W.S. Sanders, J.S. Warner, D.B. Miracle, Intermetallics 14 (2006) 348–351.

[54] H.W. Yang, P. Dong, J.Q. Wang, Y. Li, Mater. Sci. Eng. A 449–451 (2007) 273–276.